Supplemental Data

A New Model for Asymmetric Spindle Positioning in Mouse Oocytes

Melina Schuh and Jan Ellenberg

Supplemental Experimental Procedures

Measurement of the cytoplasmic actin filament length

To measure the average filament length between two nodes in the cytoplasmic actin network, we recorded 3D-stacks of oocytes stained with Alexa488-phalloidin (40-50 optical sections, 0.2 µm spacing) (Movie S1). In these stacks, the filament length between two nodes or between a node and the end of the filament in the cytoplasm was measured interactively with ImageJ (http://rsb.info.nih.gov/ij/). Representative examples are shown in Figure S1

Automated 3D tracking of spindle relocation, bead dynamics and manual tracking of actin nodes

To measure the kinetics of spindle relocation we injected oocytes with mRNA encoding EGFP-MAP4 to label microtubules. We then recorded z-stacks of the entire oocyte volume during spindle relocation using an autofocussing macro [1]. We corrected for drifts during image acquisition with the ‘correct drift’ function of Imaris (Bitplane) after segmenting the oocyte volume by low thresholding on the soluble EGFP-MAP4 pool.

Afterwards we segmented the spindle by applying a higher threshold and tracked the spindle's center of mass during relocation using Imaris.

For averaging of spindle relocation in different oocytes, we temporally aligned the different data sets to the time when the spindle slowed down due to arrival at the cortex. In ML-7 treated oocytes, where the spindle did not reach the cortex (Figure 3E), the data sets were aligned to identical time points after the beginning of image acquisition. The distance of the spindle to the alignment position was calculated for each time point by processing the spindle coordinates in Excel and plotted over time. To calculate average velocities of spindle relocation, the spindle velocity in each oocyte was calculated by linear regression analysis of the displacement plots. Average, standard deviation, and statistical significance based on Student's t-test were calculated in Excel. To measure the delay between bipolar spindle formation and spindle relocation, we recorded 3D data sets of spindle formation and subsequent relocation in live mouse oocytes. Once a bipolar spindle had formed, we determined the degree of spindle eccentricity by measuring the distance of the two spindle poles from the cortex, and by calculating the ratio between the proximal and the distal value. In addition, we measured the delay between bipolar spindle formation and the onset of spindle relocation. The results are plotted in Figure 4E.

Beads were automatically tracked during spindle relocation in 4D data sets of oocytes injected with fluorescent beads using drift correction, segmentation and tracking in Imaris.

Actin nodes were tracked interactively using the ManualTracking Plugin for ImageJ.

References

1. Rabut, G., and Ellenberg, J. (2004). Automatic real-time three-dimensional cell tracking by fluorescence microscopy. J Microsc *216*, 131-137.
2. Schuh, M., and Ellenberg, J. (2007). Self-organization of MTOCs replaces centrosome function during acentrosomal spindle assembly in live mouse oocytes. Cell *130*, 484-498.

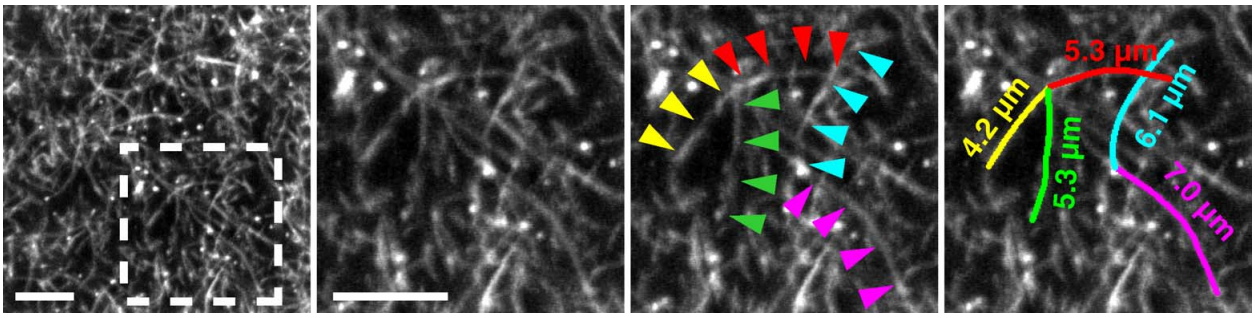

Figure S1. 3D structure of the cytoplasmic actin network.

Oocytes were fixed during spindle relocation and stained with Alexa-488-phalloidin to label F-actin. Z-projections (4 sections, every 0.2 µm) are shown. Boxed region is magnified next to overview image. Colored arrowheads highlight actin filaments between branch points. The length of these filaments in specified in the last image. Scale bar: 5 µm. The corresponding complete z-stack of the actin network is shown in Movie S1.

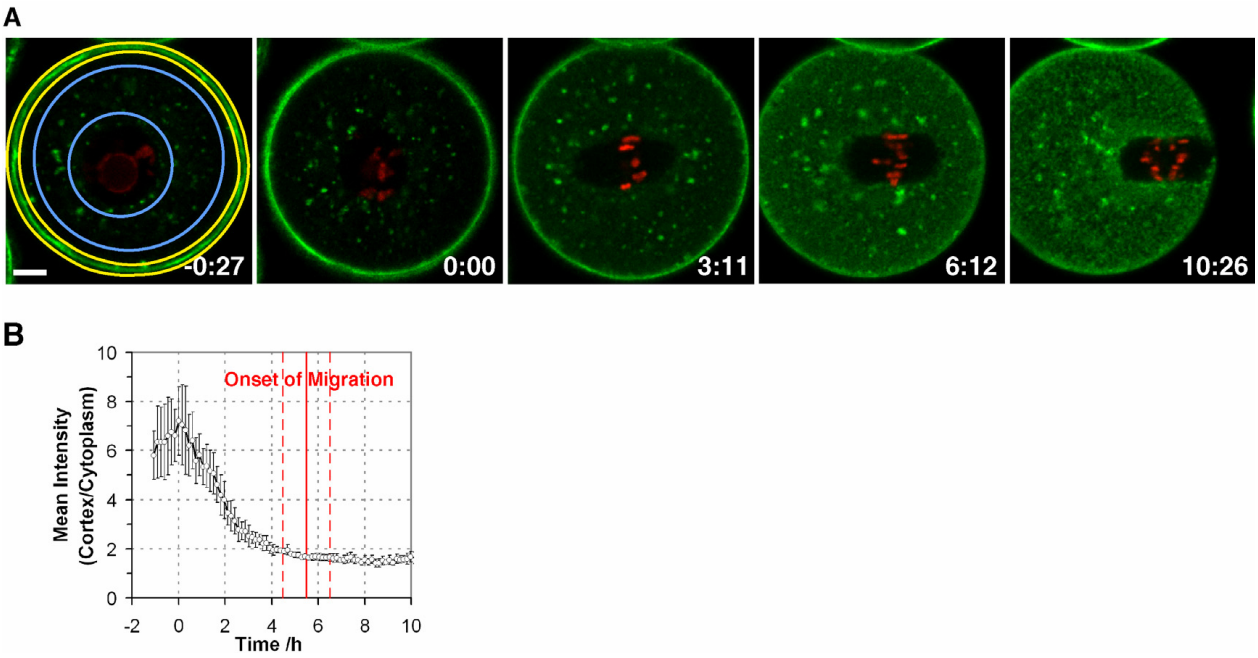

Figure S2. Fmn2-EGFP localizes at the cortex of mouse oocytes and translocates into the cytoplasm before spindle migration.

(A) Time-lapse imaging of a maturing oocyte expressing Fmn2-EGFP (green) and H2B-mRFP1 (red, chromosomes). Circles highlight cortical (yellow) and cytoplasmic regions (blue) in which mean intensities were measured. Scale bar: 10 µm. Time hh:mm relative to NEBD.

(B) The ratio of the mean intensity of Fmn2-EGFP at the cortex and in the cytoplasm was determined from oocytes expressing Fmn2-EGFP and H2B-mRFP1 like in (A). In addition, the onset of spindle relocation is displayed (red line). Averages and standard deviations from five oocytes are shown (error bars and dashed lines).

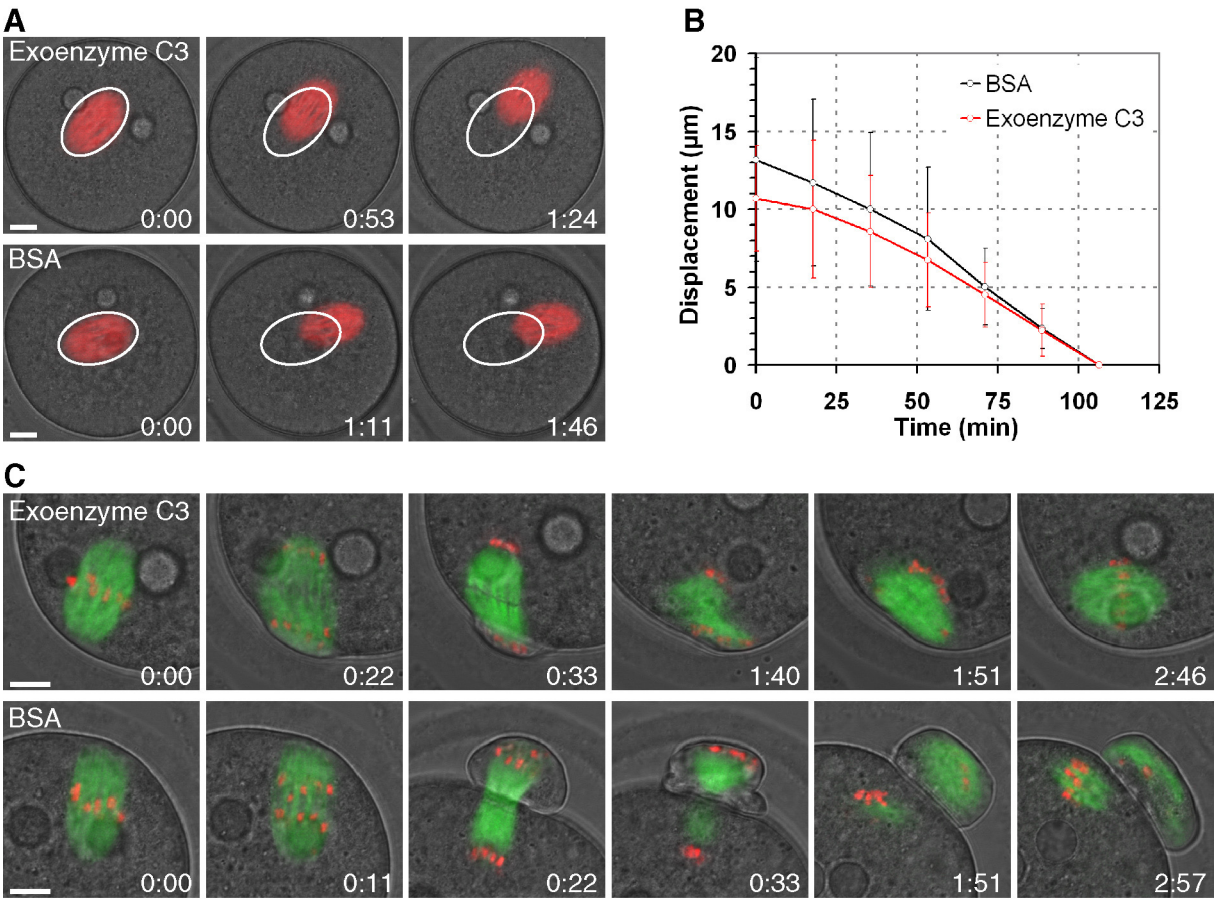

Figure S3. Spindle relocation is independent of Rho.

(A) Spindle relocation in live oocytes expressing EGFP-MAP4 (red, microtubules, merged with DIC). Oocytes were injected with 120 nM final concentration exoenzyme C3 (first row) or BSA (second row). White oval marks initial spindle position. Scale bar: 10 µm. Time hh:mm.

(B) The spindle was automatically tracked in BSA (black curve; v=0.12±0.05 µm/min; n=6) or 120 nM exoenzyme C3 injected oocytes (red curve; v=0.12±0.03 µm/min; n=6) in 3D data sets (13 sections, every 6 µm) as shown in (A). The velocity of spindle relocation was not significantly affected by exoenzyme C3 injection (p=0.94). Both curves represent averages and standard deviations from 6 oocytes.

(C) Chromosome segregation in live oocytes expressing EGFP-MAP4 (green, microtubules) and H2B-mRFP1 (red, chromosomes). Oocytes were injected with 120 nM exoenzyme C3 (upper row) or BSA (lower row). Cytokinesis failed in 22/22 oocytes that

were injected with exoenzyme C3, confirming that Rho was inhibited. Scale bar: 10 µm. Time hh:mm.

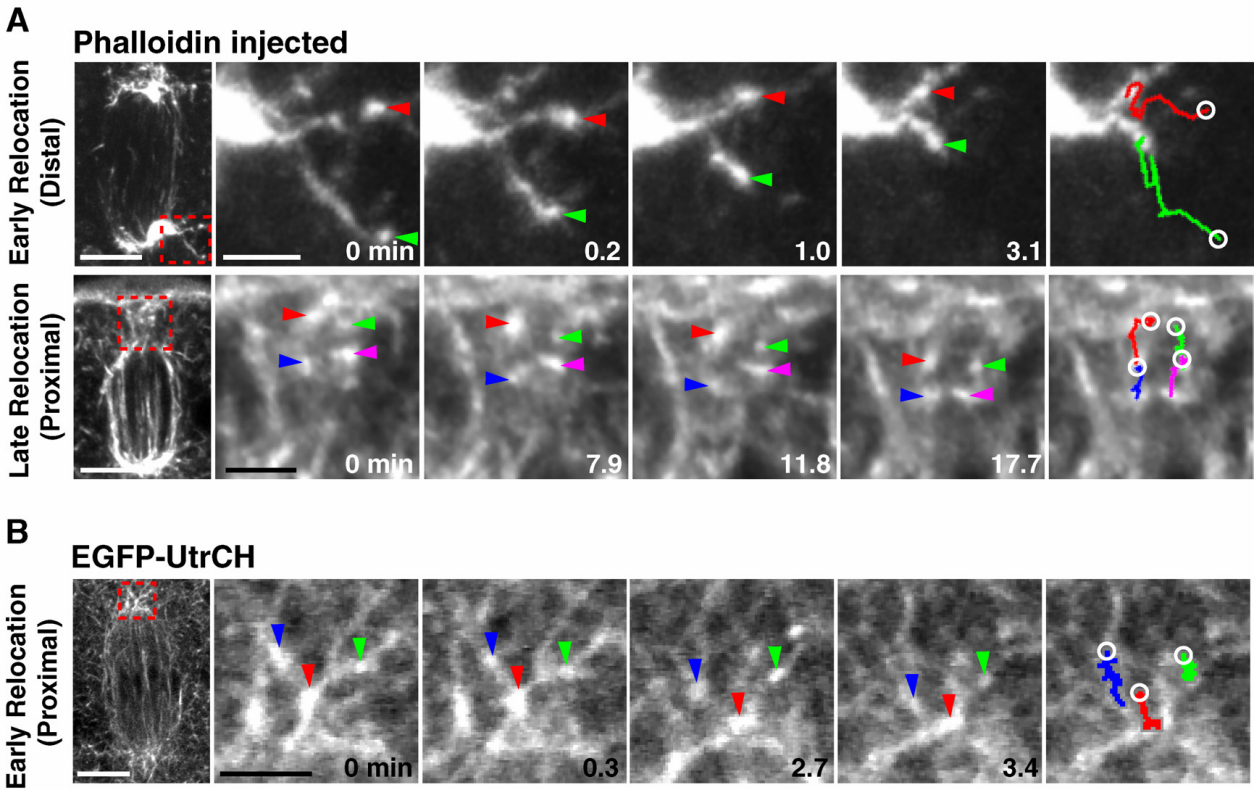

Figure S4. Actin nodes are pulled to both spindle poles during early and late relocation.

(A) TMR-phalloidin labeled actin filaments during early (first row) and late spindle relocation (second row; same oocyte as in Figure 2A). Boxed regions at the distal (upper row) or proximal pole (lower row) are magnified next to overviews. Colored arrowheads highlight relative positions of actin nodes. Tracks are superimposed on last images. Circles mark initial positions. Scale bars overview: 10 µm; magnification: 3 µm.

(B) EGFP-UtrCH labeled actin filaments during early spindle relocation. Boxed region is magnified next to overview. Colored arrowheads highlight relative positions of actin nodes. Tracks are superimposed on last image. Circles mark initial positions. Scale bars overview: 10 µm; magnification: 3 µm.

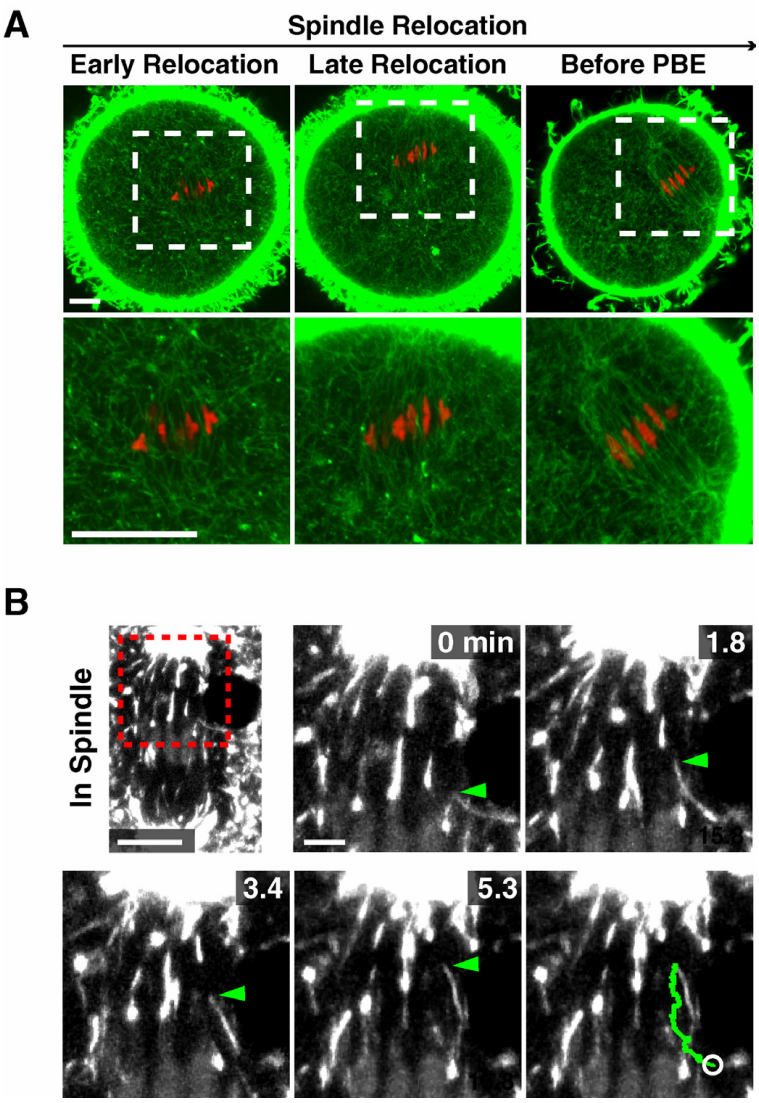

Figure S5. Actin filaments are pulled into the spindle at late stages of spindle relocation.

(A) Oocytes were fixed at indicated stages after isolation and stained with Alexa-488-phalloidin to label F-actin (green) and with Hoechst to label chromosomes (red). Boxed regions are magnified in the second row. Scale bars: 10 µm.

(B) TMR-phalloidin labeled actin filaments in the spindle region. Boxed region at the spindle periphery is magnified next to overview. Colored arrowhead highlights a filament that is pulled into the spindle. Track is superimposed on last image. Circle marks initial position. Scale bar overview: 10 µm; magnification: 3 µm.

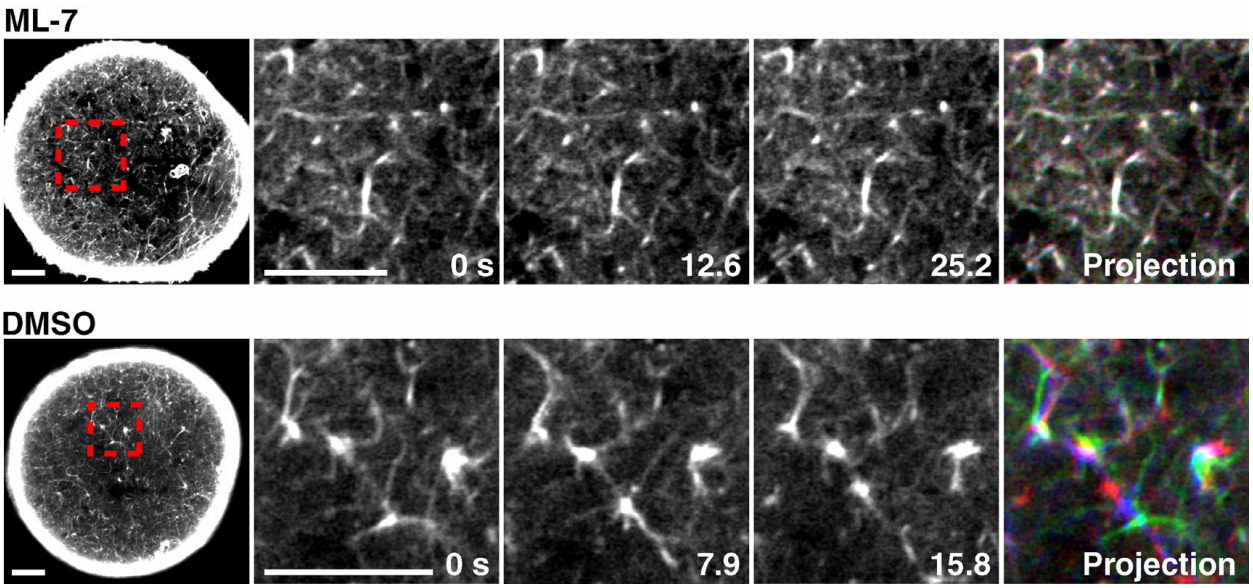

Figure S6. Actin network dynamics depend on MLCK activity.

Oocyte expressing EGFP-UtrCH (F-actin) after treatment with 15 µM ML-7 (upper row) or DMSO (lower row). Boxed regions are magnified next to overview. Projections are time-colored in RGB. Scale bars: 10 µm.

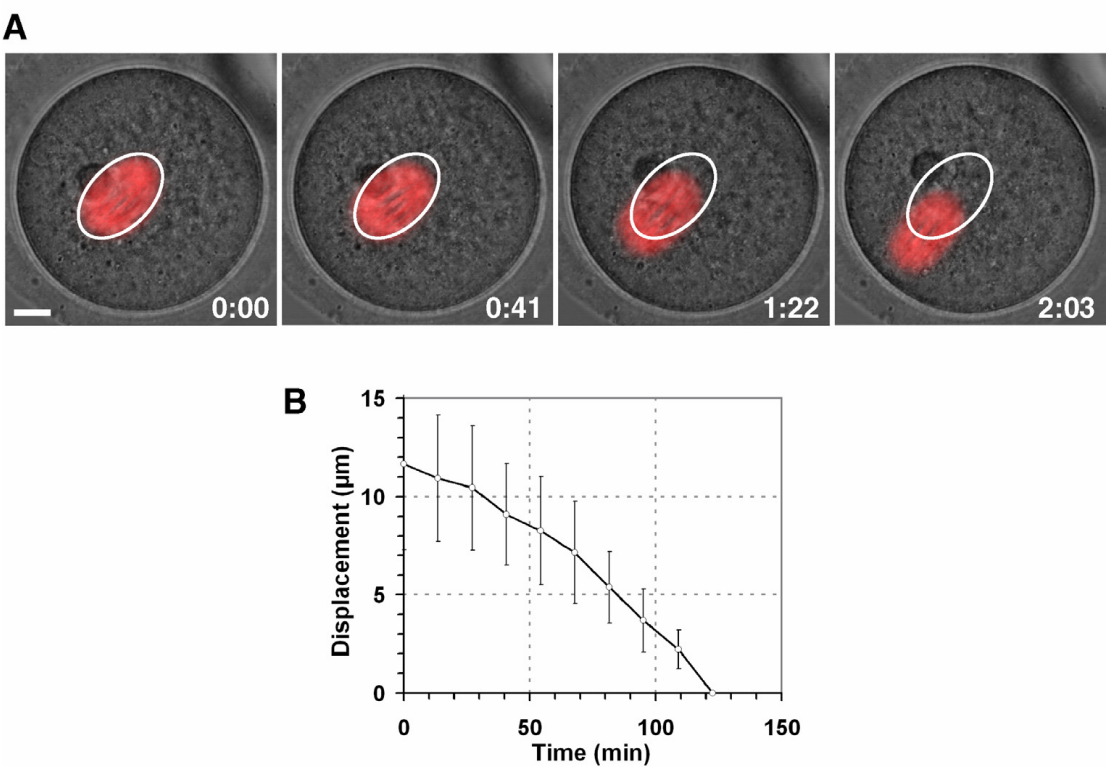

Figure S7. The spindle accelerates during relocation.

(A) Spindle relocation in a live oocyte expressing EGFP-MAP4 (red, microtubules) merged with DIC. White oval marks initial spindle position. Scale bar 10 µm. Time hh:mm.

(B) Spindles were tracked in 4D data sets (13 sections, every 6 µm) as shown in (A). The distance of the spindle to the position where it slows down due to arrival at the cortex is plotted over time. Averages and standard deviation of 15 oocytes are shown.

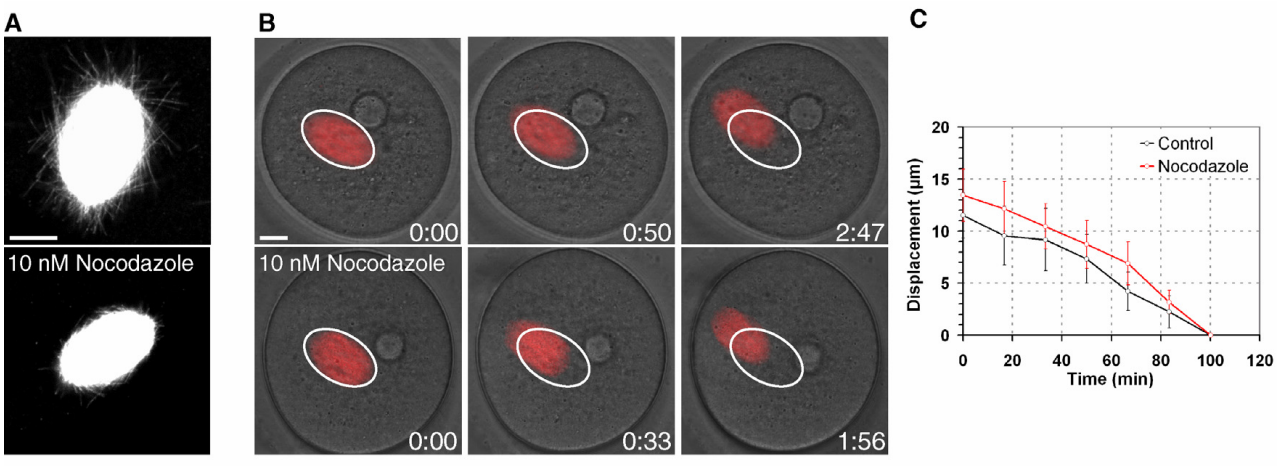

Figure S8. Astral-like microtubules are dispensable for spindle relocation.

(A) Immunofluorescence of tubulin in control oocyte (upper panel) and oocyte treated with 10 nM nocodazole after the onset of spindle relocation (lower panel).

(B) Spindle relocation in live oocytes expressing EGFP-MAP4 (red, microtubules) merged with DIC. Oocytes in lower row were treated with 10 nM nocodazole after the onset of spindle relocation (lower panel). White ovals mark initial spindle positions. Scale bar: 10 µm. Time hh:mm.

(C) The spindle was tracked in control (black curve; v=0.11±0.01 µm/min; n=7) or 10 nM nocodazole treated oocytes (red curve; v=0.15±0.04 µm/min; n=7; p=0.09) in 3D data sets (11 sections, every 7 µm) as shown in (B). Both curves represent averages and standard deviations from 7 oocytes.

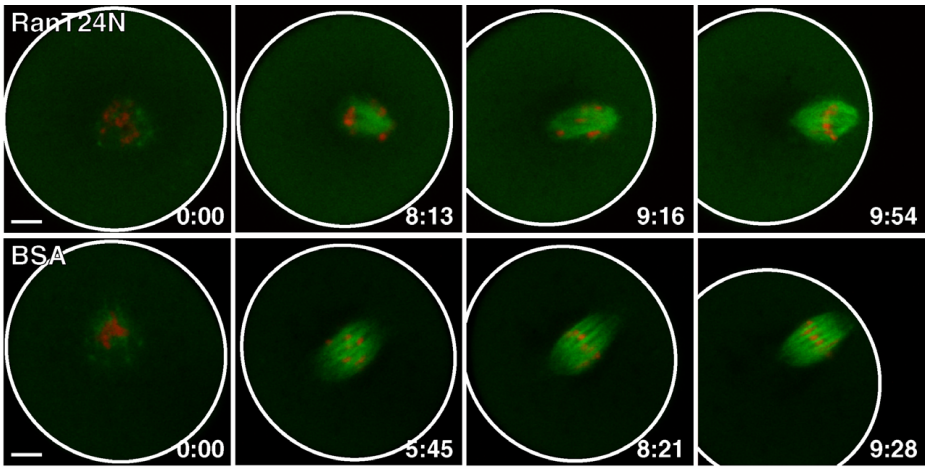

Figure S9. Spindle relocation is independent of Ran.

Spindle relocation in live oocytes expressing EGFP-MAP4 (green, microtubules) and H2B-mRFP1 (red, chromosomes). Oocytes were injected with 13 µM final concentration RanT24N (upper panel) sufficient to inhibit nucleocytoplasmic transport (data not shown, see [2]) or BSA (lower panel). The spindle relocated to the cortex in 8/10 RanT24N injected oocytes and 19/20 BSA injected oocytes. White circle marks oocyte surface. Scale bar: 10 µm. Time hh:mm.

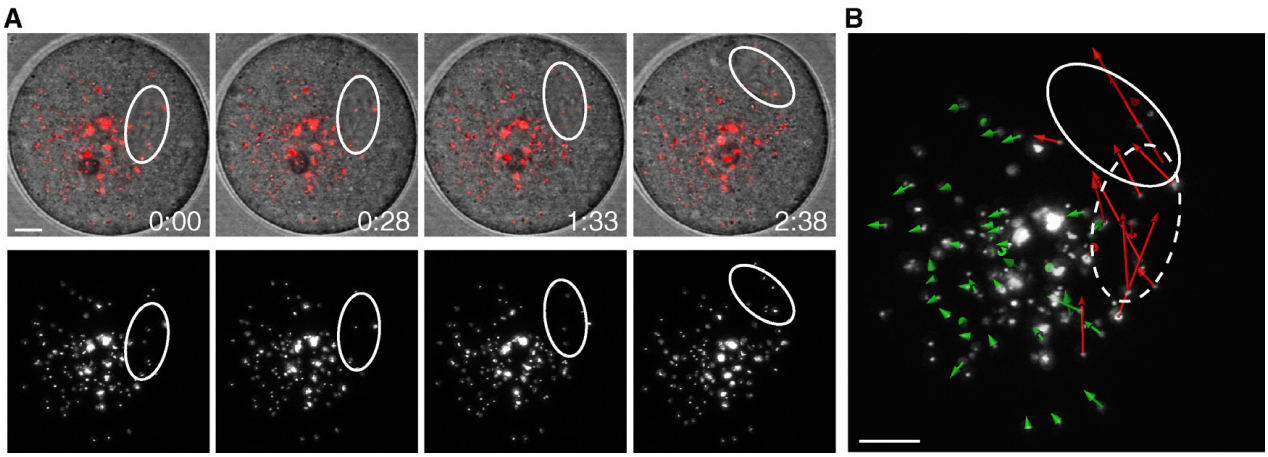

Figure S10. Cytoplasmic dynamics are restricted to the spindle region during relocation.

(A) Time-lapse imaging of fluorescent beads (0.56 µm diameter, red, projected from a z-stack of 25 sections, every 3 µm) during spindle relocation in a live oocyte; merged with DIC images (upper panel, single section), and separately (lower panel). White ovals mark spindle positions derived from DIC. Scale bar 10 µm. Time hh:mm.

(B) Arrows illustrating bead displacement in proximity (red) and distant to spindle (green) for the data set shown in (A) are superimposed on fluorescent bead signal. White ovals mark initial (dashed) and final spindle positions. Scale bar: 10 µm.

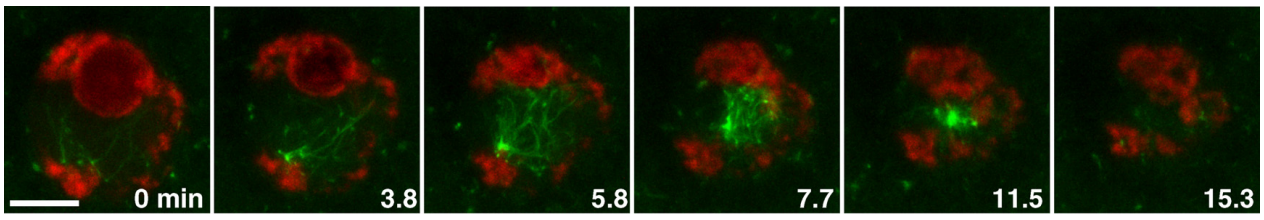

Figure S11. Contractile actin cables transiently form between the chromosomes at NEBD.

Time-lapse imaging of the nuclear region during NEBD in an oocyte expressing EGFP-UtrCH (F-actin, green) and H2B-mRFP1 (chromosomes, red). Merged projection of a z-stack is shown (13 sections, every 2 µm). Scale bar: 10 µm.